CSIRO PUBLISHING www.publish.csiro.au/journals/eg Copublished paper, please cite all three:
Exploration Geophysics, 2008, **39**, 60–67; *Butsuri-Tansa*, 2008, **61**, 60–67; *Mulli-Tamsa*, 2008, **11**, 60–67

Fast numerical methods for marine controlled-source electromagnetic (EM) survey data based on multigrid quasi-linear approximation and iterative EM migration*

Takumi Ueda[1,3] Michael S. Zhdanov[2]

[1]Geological Survey of Japan, National Institute of Advanced Industrial Science and Technology (AIST) Central 7 Higashi 1-1-1, Tsukuba, Ibaraki 305-8567, Japan.
[2]Department of Geology and Geophysics, University of Utah, 135 S. 1460 E., Room 719, Salt Lake City, UT 84112-0111, USA.
[3]Corresponding author. Email: takumi.ueda@aist.go.jp

Abstract. In this paper we consider an application of the method of electromagnetic (EM) migration to the interpretation of a typical marine controlled-source (MCSEM) survey consisting of a set of sea-bottom receivers and a moving electrical bipole transmitter. Three-dimensional interpretation of MCSEM data is a very challenging problem because of the enormous number of computations required in the case of the multi-transmitter and multi-receiver data acquisition systems used in these surveys. At the same time, we demonstrate that the MCSEM surveys with their dense system of transmitters and receivers are extremely well suited for application of the migration method. In order to speed up the computation of the migration field, we apply a fast form of integral equation (IE) solution based on the multigrid quasi-linear (MGQL) approximation which we have developed. The principles of migration imaging formulated in this paper are tested on a typical model of a sea-bottom petroleum reservoir.

Key words: electromagnetic method, marine CSEM, integral equation, quasi-linear approximation, electromagnetic migration, numerical method, inverse problem.

Introduction

During the past few years marine controlled-source electromagnetic (MCSEM) surveys have become widely used for offshore petroleum exploration (e.g. Eidesmo et al., 2002; Ellingsrud et al., 2002; Edwards, 2005; Constable and Weiss, 2006; Constable and Srnka, 2007). The main target of such surveys is the sub-sea-bottom petroleum reservoir, which is usually characterised by a low electrical conductivity anomaly within the relatively conductive sea-bottom sediments. There is growing interest in the interpretation of the MCSEM databased on 3D geoelectrical models.

Figure 1 demonstrates the general survey configuration of the MCSEM method.

A set of electromagnetic receivers (typically from 10 to 50) is deployed at the seafloor along the survey profile line(s). Usually, these receivers are dropped from the survey vessel and fall freely to the seafloor. There are two well known transmitter types for marine EM surveys. One is a vertical electric bipole, used in the magnetometric resistivity (MMR) method (Tada and Seama, 2006; Kasaya et al., 2006); the other is the horizontal electric current bipole transmitter. In this paper, we develop a new data interpretation method for the horizontal bipole configuration. The transmitting horizontal electric bipole typically has a length of several hundred metres and is towed by the survey vessel via an umbilical cable. This transmitter generates a low-frequency (typically from 0.1 to 10 Hz) EM field, which propagates both upwards in the sea-water and downwards within the sea bottom. The receivers measure the amplitude and the phase of the electric and/or magnetic fields generated by the transmitter. The recorded signal is formed both by the primary field from the transmitter and by the EM response from the geoelectrical structure beneath the seafloor. After data acquisition is completed, the receivers float up to the surface and are retrieved by the survey vessel.

The conventional approach, based on standard 3D forward modelling and inversion of MCSEM data, meets significant difficulties because of the enormous number of computations required in the case of the multi-transmitter and multi-receiver data acquisition systems typical for marine CSEM surveys.

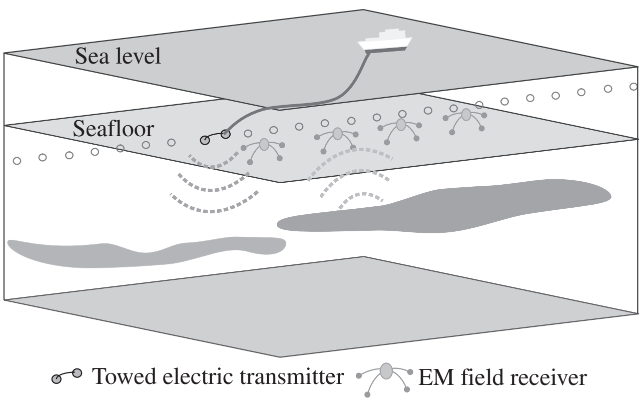

Fig. 1. The general survey configuration of the MCSEM method. An electric bipole transmitter towed by the survey vessel generates an EM signal, while fixed multi-component EM field receivers located on the seafloor measure the EM response from the geoelectrical structure beneath the seafloor.

*Part of this paper was presented at the 116th SEGJ Conference, 2007.

 10.1071/EG08002 0812-3985/08/010060

There is, however, an alternative approach to the solution of this problem, which is based on the principles of multigrid quasi-linear approximation (MGQL) of integral equation (IE) modelling and electromagnetic (EM) holography and migration. There are several papers on EM holography and migration; see for example, Zhdanov and Frenkel (1983*a*, *b*), Zhdanov and Keller (1994), Zhdanov et al. (1996), Zhdanov and Traynin (1997), Zhdanov (1981, 1999, 2001, 2002), Tompkins (2004), and Mittet et al. (2005).

In this paper we consider an application of this approach to the interpretation of a typical MCSEM survey which consists of a set of seafloor receivers and a moving electrical bipole transmitter. The receivers record the magnitude and the phase of the frequency domain (FD) EM field generated by the moving transmitter and scattered back by sea-bottom geoelectrical structures. The combined EM signal in the receivers forms a broad-band EM hologram of the sea-bottom geological target (e.g. petroleum reservoir). In order to reconstruct the geoelectrical image of the target, we replace the set of receivers with a set of auxiliary transmitters located at the receivers' positions. The strength and the phase of the signals transmitted by these auxiliary transmitters are determined from the fields observed in the receivers. These transmitters generate an EM field which is called the backscattering or the migration field. The background/migration EM fields include geoelectrical information about the seafloor, because their transmitter signal is based on the observed field. The vector cross-power spectrum of the background field (the field generated by the original transmitter in a medium without a target) and backscattering field produces a numerical reconstruction of a volume image of conductivity distribution (Zhdanov, 2001).

We should note, however, that the frequency of the EM signal used in the marine EM field is very low, ~1 Hz. In this low frequency range, the EM field propagates in sea-bottom formations according to the diffusion equation (Zhdanov and Keller, 1994), which results in relatively low resolution of the geoelectrical image obtained by the numerical algorithm described above. In order to improve the resolution of the EM holographic imaging, we should apply the migration iteratively. In this paper we present a description of the corresponding method of iterative migration, using the MGQL method with application to the MCSEM data.

MGQL of the IE method

For completeness, we begin our paper with a short review of the MGQL method (Ueda and Zhdanov, 2006). In the framework of the QL approximation we formulate a general forward EM problem so that the anomalous conductivity can be treated as a perturbation from a known background (or 'normal') conductivity distribution. The solution of the EM problem in this case contains two parts:

1) the linear part, which can be interpreted as a direct scattering of the source field by the inhomogeneity without taking into account coupling between scattering (excess) currents, and
2) the non-linear part, which is composed of the combined effects of the anomalous conductivity and the unknown scattered field in the inhomogeneous structure.

The QL approximation is based on the assumption that this last part is linearly proportional to the background field $\mathbf{E}^b$ through some electrical reflectivity tensor $\hat{\lambda}(\mathbf{r})$ (Zhdanov and Fang, 1996):

$$\mathbf{E}^a(\mathbf{r}) \approx \hat{\lambda}(\mathbf{r})\mathbf{E}^b(\mathbf{r}). \tag{1}$$

A simple modification of this equation was introduced by Gao et al. (2004) for 3D EM modelling in anisotropic formations for well logging applications. They assumed that the anomalous field is linearly proportional to the absolute value of the background field:

$$\mathbf{E}^a(\mathbf{r}) \approx \lambda(\mathbf{r})|\mathbf{E}^b(\mathbf{r})|. \tag{2}$$

where $\lambda(\mathbf{r}) = (\lambda_x, \lambda_y, \lambda_z)$ is an electrical reflectivity vector.

Note that exact representation (2) always exists because the corresponding electrical reflectivity vector can always be found for any given anomalous and background electric fields. Formula (2) becomes an approximation if we use some approximate method (for example, a multigrid approach introduced by Ueda and Zhdanov (2006)) for evaluation of the electrical reflectivity vector. In the framework of the multigrid approach, the components of the electrical reflectivity vector on a coarse grid are found by direct calculations as:

$$\begin{aligned} \lambda_x(\mathbf{r}_c) &= \mathbf{E}^a_x(\mathbf{r}_c)/|\mathbf{E}^b(\mathbf{r}_c)|, \\ \lambda_y(\mathbf{r}_c) &= \mathbf{E}^a_y(\mathbf{r}_c)/|\mathbf{E}^b(\mathbf{r}_c)|, \\ \lambda_z(\mathbf{r}_c) &= \mathbf{E}^a_z(\mathbf{r}_c)/|\mathbf{E}^b(\mathbf{r}_c)|, \end{aligned} \tag{3}$$

assuming that $|\mathbf{E}^b(\mathbf{r}_c)| \neq 0$.

After we have found $\lambda(\mathbf{r}_c)$, we introduce a fine discretisation grid $\sum_f$ describing the conductivity distribution in the same model. We determine the $\lambda(\mathbf{r}_f)$ values on this new grid by linear interpolation (where $\mathbf{r}_f$ denotes the centres of the cells of the grid $\sum_f$ with fine discretisation). We compute the anomalous electric field $\mathbf{E}^a(\mathbf{r}_f)$ in the centres of the cells of the new grid $\sum_f$ with fine discretisation using expression (2):

$$\mathbf{E}^a(\mathbf{r}_f) \approx \lambda(\mathbf{r}_f)|\mathbf{E}^b(\mathbf{r}_f)|. \tag{4}$$

We can find now the total electric field $\mathbf{E}(\mathbf{r}_f)$ on a new grid, as:

$$\mathbf{E}(\mathbf{r}_f) = \mathbf{E}^a(\mathbf{r}_f) + \mathbf{E}^b(\mathbf{r}_f). \tag{5}$$

Finally, we compute the observed fields in the receivers using the discrete analogue of the IE form of Maxwell's equations for the grid with fine discretisation. In the next section, we will demonstrate a numerical comparison between the full IE and MGQL methods.

Comparison between the full IE and MGQL modelling results

A detailed numerical study of the multi-grid-based QL approximations was presented in the paper by Ueda and Zhdanov (2006). In this section, we present the results of another study, which illustrates different aspects of the MGQL method.

In this set of numerical experiments we have investigated more carefully the errors which could appear in the MGQL modelling of the typical 2D MCSEM survey where the data in the sea-bottom receiver are collected from the different transmitters moving along a line above this receiver. A vertical cross-section of the model is shown in Figure 2.

The sea-bottom reservoir with a resistivity of 100 Ω.m, a thickness of 0.1 km, and a horizontal size of 5 km by 5 km is located at a depth of 1 km below the sea bottom, within a homogeneous conductive background with a resistivity of 1 Ω.m. The synthetic MCSEM survey was conducted with a set of horizontal electric dipole transmitters moving at an elevation 50 m above the seabed. The separation between the different transmitter positions is 200 m. The horizontal E_x component of the electric field generated by the transmitters is recorded by an array of seafloor electric receivers located 5 m above the

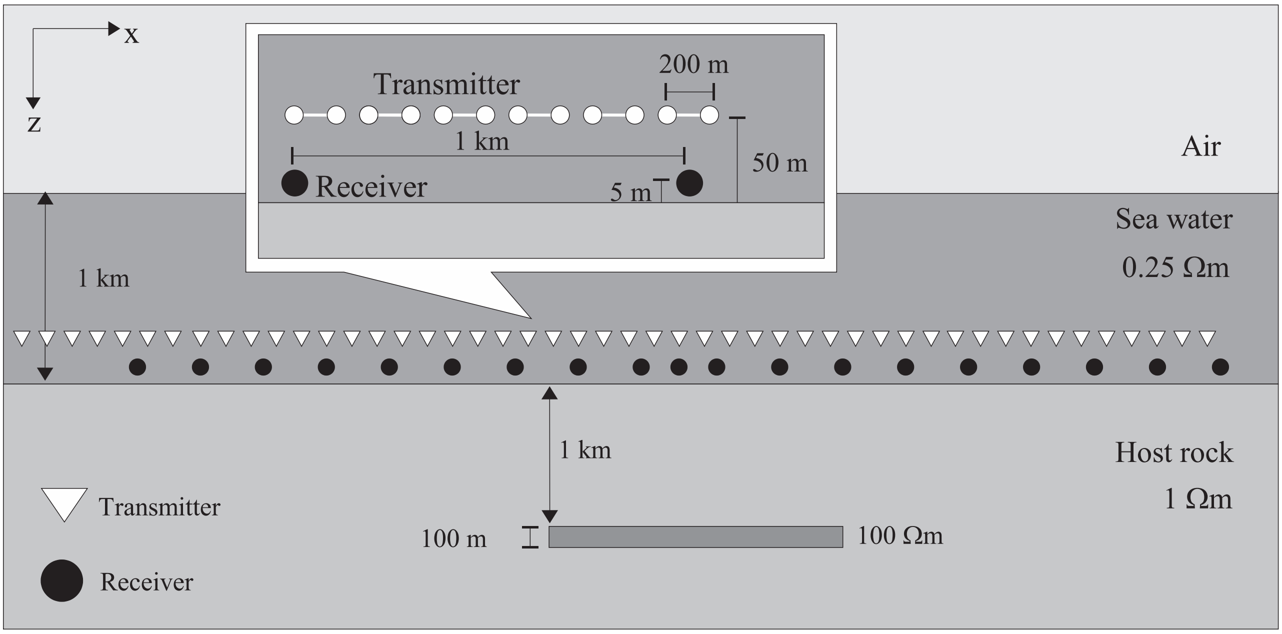

Fig. 2. A typical 2D MCSEM survey where the data are collected from the different transmitters moving along a horizontal line above the sea-bottom receivers.

sea bottom along the same line, with the separation between receivers of 1 km.

Numerical modelling was conducted using the rigorous IE and the MGQL methods (Hursán and Zhdanov, 2002). The reservoir was divided into $50 \times 50 \times 2 = 5000$ cells, with a cell size of 0.1 km by 0.1 km by 0.05 km in the x, y, and z directions, respectively. This grid was used for the rigorous IE modelling. We used a coarse grid, consisting of $25 \times 25 \times 2 = 1250$ cells, with a cell size of 0.2 km by 0.2 km by 0.05 km, for the MGQL modelling.

Figures 3 and 4 present the observed MCSEM data for different receivers computed using the rigorous IE method and the MGQL approximation respectively. In all plots the origin of the horizontal coordinates corresponds to the receiver position, while the relative horizontal location of the reservoir is shown schematically by the bold horizontal bar. The top panels in these figures present the amplitude-versus-offset (AVO) curves of the total electric field and the field normalised by the background electric field. The AVO curve for the total field computed by the rigorous IE method is shown by the solid line, while the MGQL solution is plotted by the filled circles. The dashed line shows the AVO curve for the normalised field obtained with the IE code, while the open circles represent the same data computed by the MGQL method.

The bottom panels in the same figures show the absolute values of the difference between the IE and MGQL solutions normalised by the IE solution. The solid line corresponds to the log scale, while the solid line with dots is plotted on a linear scale, for convenience. One can see that the maximum values of the differences (errors of the MGQL approximation) do not exceed 3%. For the synthetic model experiment described above, the MGQL calculation was approximately four times faster than the

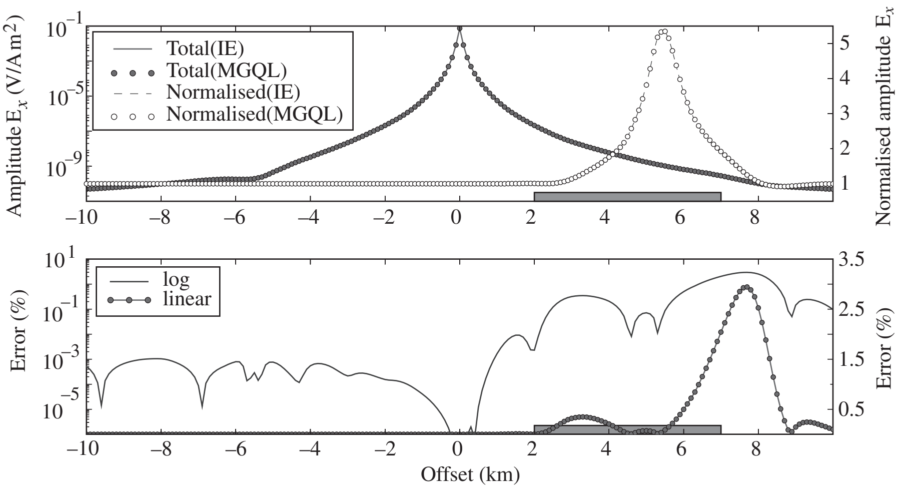

Fig. 3. The top panel presents the amplitude-versus-offset (AVO) curves of the total electric field (a solid line for the IE solution and filled circles for the MGQL solution) and an AVO curve of the field normalised by the background electric field (a dashed line shows the AVO curve for the normalised field obtained with the IE code, while the open circles represent the same data computed by the MGQL method). The bottom panel shows the absolute values of the difference between the IE and MGQL solutions normalised by the IE solution. The reservoir is located from 2 to 7 km in the x direction.

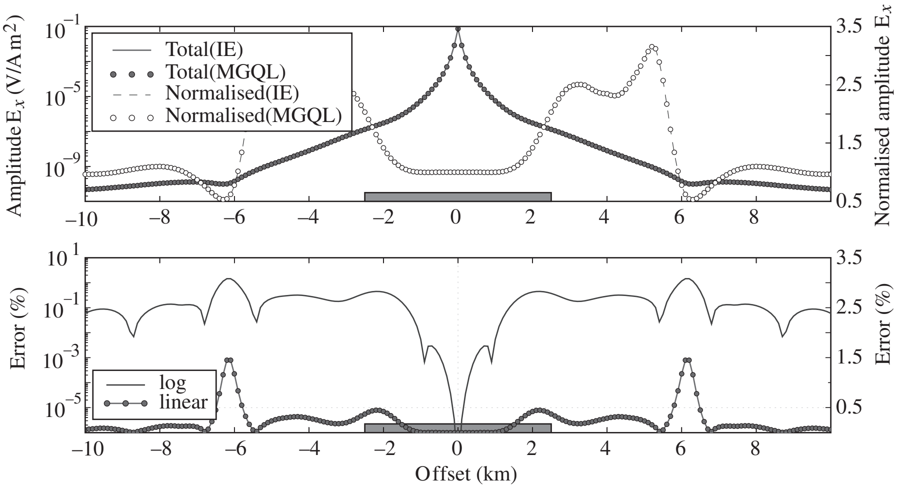

Fig. 4. The top panel presents the amplitude-versus-offset (AVO) curves of the total electric field (a solid line for the IE solution and filled circles for the MGQL solution) and an AVO curve of the field normalised by the background electric field (the dashed line shows the AVO curve for the normalised field obtained with the IE code, while the open circles represent the same data computed by the MGQL method). The bottom panel shows the absolute values of the difference between the IE and MGQL solutions normalised by the IE solution. The reservoir is located from −2.5 to 2.5 km in the x direction.

calculation by the IE method. The computer memory required for the MGQL simulation is approximately 10 times less than that for the IE method. This numerical study demonstrates the accuracy of the developed fast-modelling technique based on the MGQL method.

EM migration of the MCSEM data

Principles of EM migration

In this section, we will formulate the basic principles of EM migration (Zhdanov, 2002) applied to the interpretation of the MCSEM data. Let us consider a typical MCSEM survey consisting of a set of electric field receivers located at the sea bottom, and an electric bipole transmitter moving at some elevation above the sea bottom, as shown in Figure 2. We assume that the electrical conductivity in the model can be represented as a sum of a background conductivity $\sigma = \sigma_b$ and an anomalous conductivity $\Delta\sigma$ distributed within some local inhomogeneity D associated with the location of the petroleum reservoir. The background conductivity is formed by a horizontally layered model consisting of nonconductive air, a conductive seawater layer, and a horizontally homogeneous (layered) section of a sea-bottom formation (Figure 2).

The receivers are located at the points with radius-vector $\mathbf{r}_j$, $(j = 1, 2, 3, \ldots, J)$ in some Cartesian coordinate system. Every receiver $\mathbf{R}_j$ records electric and magnetic field components of the field generated by an electric bipole transmitter moving above the receivers. We denote this field as $\mathbf{E}_i(\mathbf{r}_i)$, $\mathbf{H}_i(\mathbf{r}_i)$ where i is the index of the corresponding transmitter, T_i, located at the point $\mathbf{r}_i$, $(i = 1, 2, 3, \ldots, I)$.

Let us consider the data observed by one receiver, $\mathbf{R}_j$. According to the reciprocity principle (Zhdanov, 2002, p. 226), one can substitute a reciprocal survey configuration for the original survey, assuming that we have electric, $\mathbf{T}_j^E$, and magnetic, $\mathbf{T}_j^H$, dipole transmitters located in the position of the receiver, $\mathbf{R}_j$, and a set of receivers measuring the reciprocal electric fields, $\mathbf{E}_j^E(\mathbf{r}_i)$ and $\mathbf{E}_j^H(\mathbf{r}_i)$, in the positions of the original transmitters, $\mathbf{T}_i$.

We can calculate now the backscattering (or migration) field for the data collected by one fixed sea-bottom receiver, $\mathbf{R}_j$. Consider, for example, the reciprocal electric field $\mathbf{E}_j^E(\mathbf{r}_i)$. This field can be represented as a sum of the background and anomalous parts:

$$\mathbf{E}_j^E(\mathbf{r}_i) = \mathbf{E}_j^b(\mathbf{r}_i) + \mathbf{E}_j^{E_a}(\mathbf{r}_i), \tag{6}$$

where the background electric field, $\mathbf{E}_j^b(\mathbf{r}_i)$, is generated by the electric dipole transmitter $\mathbf{T}_j^E$ in a model with a given background conductivity σ_b. The residual electric field, $\mathbf{R}_{Ej}(\mathbf{r}_i)$ is equal to the difference between the background and 'observed' reciprocal field:

$$\mathbf{R}_{E_j}(\mathbf{r}_i) = \mathbf{E}_j^b(\mathbf{r}_i) - \mathbf{E}_j^E(\mathbf{r}_i) = -\mathbf{E}_j^{E^a}(\mathbf{r}_i). \tag{7}$$

According to the definition (Zhdanov, 2002), the backscattering (migrated) residual field is a field generated in the background medium by a combination of all electric dipole transmitters located at points $\mathbf{r}_i$ with the current moments determined by the complex conjugate residual field $\mathbf{R}_{Ej}^*(\mathbf{r}_i)$ according to the following formula:

$$\mathbf{E}_j^m(\mathbf{r}) = \mathbf{E}_j^m(\mathbf{r}; \mathbf{R}_{E_j}^*) = \sum_{i=1}^{I} \mathbf{G}_E(\mathbf{r}|\mathbf{r}_i)\mathbf{R}_{E_j}^*(\mathbf{r}_i), \tag{8}$$

where the lower subscript j shows that we migrate the field observed by the receiver $\mathbf{R}_j$, $\mathbf{G}_E$ is the electric Green's tensor for the layered (background) conductivity model σ_b and $\mathbf{r}$ denotes the arbitrary location inside the anomalous domain. Therefore, the migration field can be computed as a superposition of 1D responses weighted by the corresponding receiver residual. It is generated by electric dipoles with unit moments located at every transmitter position in the model with the background conductivity σ_b. This 1D modelling of the field generated by electric dipole is a very fast process, which results in a fast migration algorithm.

Formula (8) allows us to reconstruct the migration field everywhere in the medium under investigation. It can be shown that this transformation is stable with respect to noise in the observed data (Zhdanov et al., 1996). At the same time the spatial distribution of the migration field is closely related to the conductivity distribution in the medium. However, one needs to apply the corresponding imaging conditions to enhance the conductivity image produced by the EM migration (Zhdanov, 2002).

In a general case of multiple receivers, the migration field is generated in the background medium by all electric dipole transmitters located above all receivers, $\mathbf{R}_j$, having the current moments determined by the complex conjugate residual field $\mathbf{R}^*_{Ej}(\mathbf{r}_i)$:

$$\mathbf{E}^m(\mathbf{r}) = \sum_{j=1}^{J}\sum_{i=1}^{I} \mathbf{G}_E(\mathbf{r}|\mathbf{r}_i)\mathbf{R}^*_{E_j}(\mathbf{r}_i). \tag{9}$$

According to formula (8), we have:

$$\mathbf{E}^m(\mathbf{r}) = \sum_{j=1}^{J} \mathbf{E}^m_j(\mathbf{r}). \tag{10}$$

Therefore, the total migration field for all receivers can be obtained by summation of the corresponding migration field computed for every individual receiver.

Regularised iterative migration

We can now apply a general scheme of the re-weighted regularised conjugate gradient method in the space of the weighted parameters (Zhdanov, 2002, p. 163), to form an iterative process for electromagnetic migration. According to this scheme, we introduce a space of weighted conductivities:

$$\sigma^w = W_m\sigma, \tag{11}$$

where the weighting operator W_m is the linear operator corresponding to multiplication of the anomalous conductivity $\Delta\sigma(\mathbf{r})$ by the function $W_m(\mathbf{r})$ equal to the square root of the integral sensitivity.

The general iterative process can be described by the formulae:

$$\sigma^w_{n+1} = \sigma^w_n + \delta\sigma^w_n = \sigma^w_n - k^\alpha_n \tilde{\mathbf{l}}^\alpha_w(\sigma^w_n), \tag{12}$$

where

$$\tilde{\mathbf{l}}^\alpha_w(\sigma^w_n) = \tilde{\mathbf{l}}^\alpha_{wn} = \mathbf{l}^\alpha_{wn} + \beta^\alpha_n \tilde{\mathbf{l}}^\alpha_{w(n-1)}, \quad \tilde{\mathbf{l}}^\alpha_{w0} = \mathbf{l}^\alpha_{w0}, \tag{13}$$

$$\beta^\alpha_n = ||\mathbf{l}^\alpha_{wn}||^2/||\mathbf{l}^\alpha_{w(n-1)}||^2, \tag{14}$$

and k_n is a step length.

The weighted regularised gradient direction at the nth iteration $\mathbf{l}^\alpha_{wn}$ can be calculated by a formula:

$$\mathbf{l}^\alpha_{wn} = W_m^{-1}\mathbf{l}_n + \alpha(\sigma^w_n - \sigma^w_{apr}), \tag{15}$$

where $\mathbf{l}_n$ is a gradient direction at the nth iteration,

$$\mathbf{l}_n = \mathrm{Re}\Sigma_{\omega n}(\tilde{\mathbf{E}}_n \cdot \tilde{\mathbf{E}}^m_n). \tag{16}$$

The fields $\tilde{\mathbf{E}}_n$ and $\tilde{\mathbf{E}}^m_n$ are determined from the following conditions. The field $\tilde{\mathbf{E}}_n$ is a combination of the electric field $\mathbf{E}_{nj}(\mathbf{r}_i)$ generated by the electric dipole transmitters T^E_j in a model with the anomalous conductivity σ_n found on the iteration number n.

The field $\tilde{\mathbf{E}}^m_n$ is obtained by the migration of the weighted residual field found on the iteration number n:

$$\tilde{\mathbf{E}}^m_n(\mathbf{r}) = \mathbf{E}^m(\mathbf{r}; W^*_d W_d \tilde{\mathbf{R}}_{nE}), \tag{17}$$

where

$$\tilde{\mathbf{R}}_{nE}(\mathbf{r}_i) = \tilde{\mathbf{E}}_n(\mathbf{r}_i) - \tilde{\mathbf{E}}^E(\mathbf{r}_i). \tag{18}$$

Note that on each step we recompute the real conductivities from the weighted conductivities at the nth iteration:

$$\sigma_n = W_m^{-1}\sigma^w_n. \tag{19}$$

Thus, we can describe the developed method of iterative migration as follows. On every iteration we calculate the theoretical electromagnetic response $\mathbf{E}^n$ for the given geoelectrical model σ_n, obtained on the previous step, calculate the residual field between this response and the observed field, $\mathbf{R}_{En}$, and then migrate the residual field. The gradient direction is computed as a sum over the frequencies of the dot product of the migrated residual field and the theoretical response $\mathbf{E}^n$. Using this gradient direction and the corresponding value of the optimal length of the step k_n (Zhdanov, 2002), we calculate the new geoelectrical model σ_n on the basis of expressions (12) and (13). The iterations are terminated when the residual reaches the level of the noise. The optimal value of the regularisation parameter α is selected using conventional principles of regularisation theory, described in Zhdanov (2002).

For marine hydrocarbon exploration, we usually seek the highly resistive hydrocarbon-filled reservoir, which is a thin and flat structure surrounded by the conductive seafloor sediments. In such a situation, it is important to obtain a geoelectrical model which has sharp resistivity boundaries and/or a blocky structure.

It was demonstrated in Portniaguine and Zhdanov (1999) and Zhdanov (2002) that images with sharp boundaries can be recovered by regularised inversion algorithms based on a special family of stabilising functionals. In particular, the minimum support (MS) functional was found to be useful in the solution of this problem. It selects the inverse model within the class of models with a minimum volume of a domain with anomalous parameter distribution. This class of models describes compact objects, which are typical targets, for example, in mineral and hydrocarbon exploration. A similar approach can be applied to migration transformation by substituting the focusing stabilisers for the minimum norm functional in equation (15). We call this technique focusing iterative migration. Numerical implementation of the focusing migration is similar to that of the focusing inversion (Zhdanov, 2002).

Numerical example of synthetic MCSEM data migration

We have analysed the principles of the iterative EM migration outlined above using as an example the synthetic MCSEM data, computed for a model shown in Figure 5.

For the numerical experiment, a model with two resistive reservoirs and a wide survey configuration is tested by the

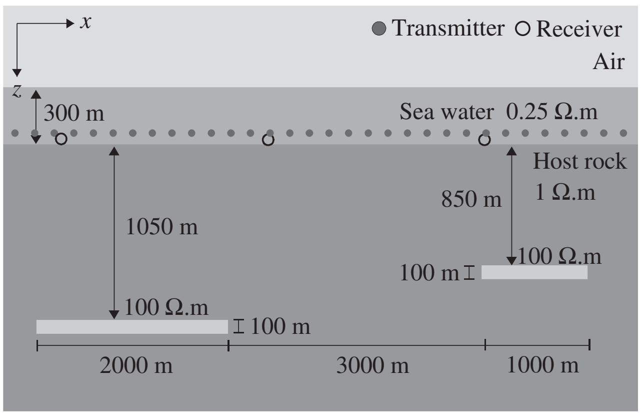

Fig. 5. A sketch of the survey and a geoelectrical model. The background layered geoelectrical model consists of a seawater layer with a thickness of 300 m, a resistivity of 0.25 Ω.m, and homogeneous sea-bottom sediments with a resistivity of 1 Ω.m. Two resistive (100 Ω.m) hydrocarbon reservoirs are located in a homogeneous sea bottom at a depth of 850 m and 1050 m below the seafloor, respectively, with a horizontal separation of 3000 m.

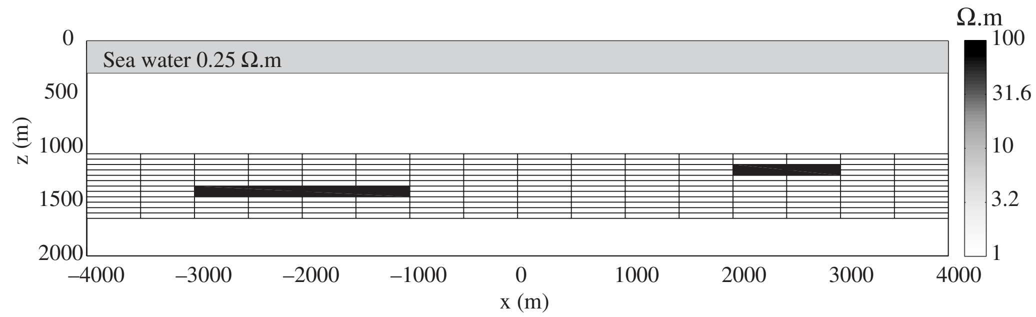

Fig. 6. A vertical cross-section of the true model.

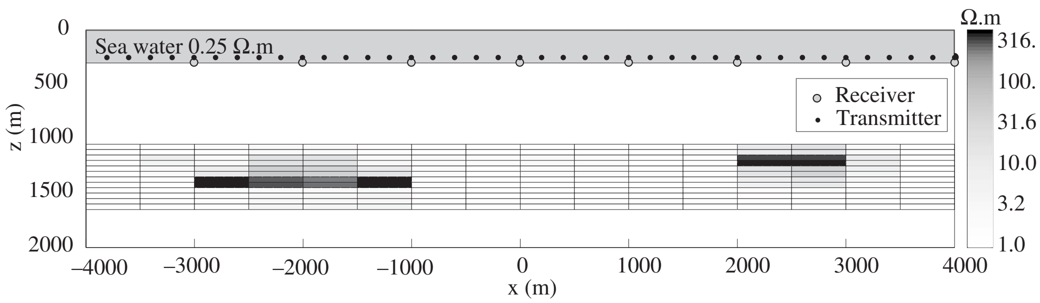

Fig. 7. A vertical cross-section of the final migration resistivity image obtained by the focusing iterative migration of noisy data.

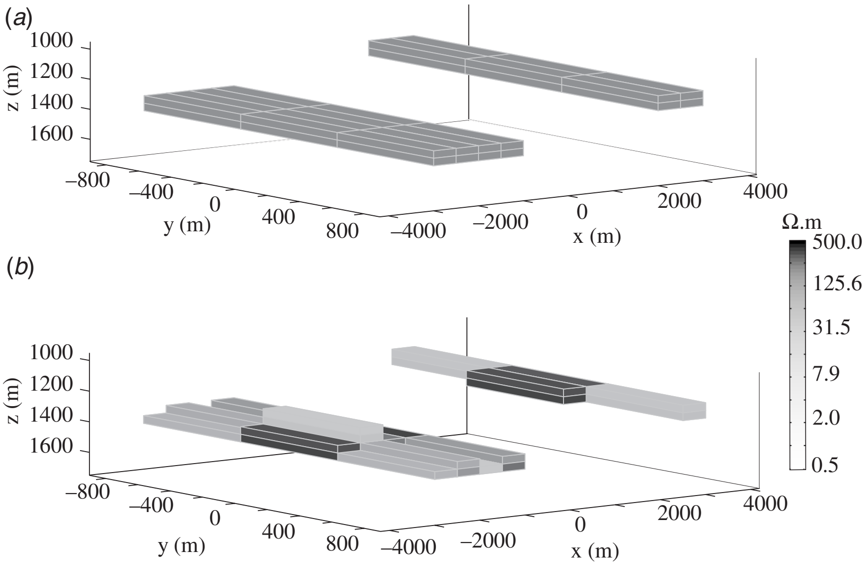

Fig. 8. A volume rendering of the true model (top panel) and iterative migration result (bottom panel). In both panels, only the cells with a resistivity higher than 10 Ω.m are plotted.

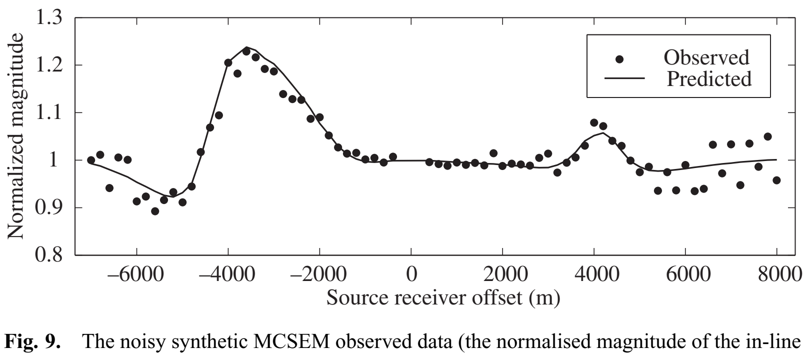

Fig. 9. The noisy synthetic MCSEM observed data (the normalised magnitude of the in-line electric field in the receivers) for transmitter #8 at a frequency of 0.25 Hz.

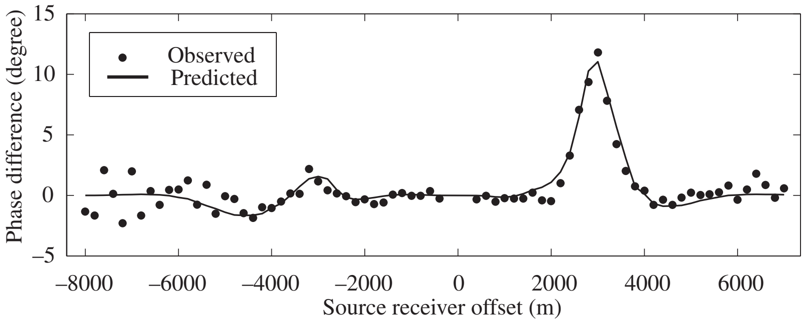

Fig. 10. The noisy synthetic MCSEM observed data (the phase difference of the in-line electric field in the receivers) for transmitter #8 at a frequency of 0.75 Hz.

developed EM migration imaging technique (Figure 5). A total of 17 seafloor receivers are deployed at the sea bottom. An electric dipole transmitter is towed along a line passing directly above the receivers at an elevation 50 m above the seafloor. The transmitter generates a frequency domain EM field every 200 m along the transmitter towing line. The separation between each receiver is 1000 m. The background layered geoelectrical model consists of a seawater layer with a thickness of 300 m, a resistivity of 0.25 Ω.m, and homogeneous sea-bottom sediments with a resistivity of 1 Ω.m.

There are two rectangular reservoirs located in the seafloor sediments at a depth of 1150 m and 1350 m below sea level, respectively. The resistivity of the reservoirs is 100 Ω.m, their thickness is 100 m, and their horizontal dimensions are 1000 m by 1000 m for the shallow reservoir and 2000 m by 1000 m for the deeper reservoir.

The area of inversion is discretised in 16 × 3 × 12 cells, and the cell sizes are 500 m, 600 m, and 50 m in the x, y, and z directions, respectively.

In order to simplify the computations, a relatively short inversion domain length in the y direction has been selected to reduce the number of the discretisation cells used in the inversion. The synthetic dataset was contaminated by artificial random noise of 1 to 10% depending on the source-receiver offset.

The iterative migration started with 10 iterations of the minimum norm (smoothing) stabiliser and then switched to the minimum support (focusing) stabiliser with seven sets of re-weighting and five iterations in each re-weighting set. We started with smoothing inversion for a stable convergence at the beginning and changed to focusing inversion to find a thin and flat hydrocarbon reservoir.

Figure 6 represents the true resistivity cross-section of this model.

Figures 7 and 8 present the 2D cross-section and 3D volume rendering of the result of iterative migration.

As one can see, the depth and the horizontal extent of the reservoir are recovered extremely well in the iterative migration result. The observed data and predicted data computed using the migration result model are plotted in Figures 9 and 10. Remember that the observed data have been contaminated by synthetic noise. The predicted data are represented by a smooth curve which fits the observed data well.

Conclusions

Electromagnetic migration was originally introduced for the interpretation of land EM data. However, this technique is most effective in the case of relatively dense EM surveys, which are difficult to implement on land. The MCSEM surveys with their dense system of transmitters and receivers are extremely well suited for the application of the migration technique. In this paper we illustrate the basic principles of EM migration in application to MCSEM data interpretation with the use of the multigrid QL approximation method.

The basic principles of the migration imaging outlined in this paper are implemented and tested on a typical model of a sea-bottom hydrocarbon reservoir. The numerical results show that migration can be treated as a prospective method of MCSEM data interpretation. Future research will be focused on the investigation of full 3D MCSEM surveys and the interpretation of MCSEM data over more complex geological targets.

Acknowledgments

The authors are thankful for the support of the Consortium for Electromagnetic Modelling and Inversion (CEMI), which includes BAE Systems, Baker Atlas Logging Services, BGP China National Petroleum Corporation, BHP Billiton World Exploration Inc., British Petroleum, Centre for Integrated Petroleum Research, EMGS, ENI S. p. A., ExxonMobil Upstream Research Co., INCO Exploration, Information Systems Laboratories, MTEM, Newmont Mining Co., Norsk Hydro, OHM, Petrobras, Rio Tinto - Kennecott, Rocksource, Russian Research Center Kurchatov Institute, Schlumberger, Shell International Exploration and Production Inc., Statoil, Sumitomo Metal Mining Co., and Zonge Engineering and Research Organization.

One of the authors (T.U.) thanks Dr T. Uchida, Dr Y. Mitsuhata, and Dr T. Yokota of the Geological Survey of Japan, AIST, for their continuous support for this paper and advice on electromagnetic exploration methods and marine EM surveys.

References

Constable, S., and Srnka, L. J., 2007, An introduction to marine controlled-source electromagnetic methods for hydrocarbon exploration: *Geophysics* **72**, WA3–WA12. doi: 10.1190/1.2432483

Constable, S., and Weiss, C. J., 2006, Mapping thin resistors and hydrocarbons with marine EM methods: insights from 1D modelling: *Geophysics* **71**, G43–G51. doi: 10.1190/1.2187748

Edwards, N., 2005, Marine controlled source electromagnetics: principles, methodologies, future commercial applications: *Surveys in Geophysics* **26**, 675–700. doi: 10.1007/s10712-005-1830-3

Eidesmo, T., Ellingsrud, S., MacGregor, L. M., Constable, S., Sinha, M. C., Johansen, S., Kong, F. N., and Westerdahl, H., 2002, Sea bed logging (SBL), a new method for remote and direct identification of hydrocarbon filled layers in deepwater areas: *First Break* **20**, 144–152.

Ellingsrud, S., Eidesmo, T., Johansen, S., Sinha, M. C., MacGregor, L. M., and Constable, S., 2002, Remote sensing of hydrocarbon layers by sea bed logging (SBL): results from a cruise offshore Angola: *The Leading Edge* **21**, 972–982. doi: 10.1190/1.1518433

Gao, G., Torres-Verdin, C., and Fang, S., 2004, Fast 3D modelling of borehole induction measurements in dipping and anisotropic formations using a novel approximation technique: *Petrophysics* **45**, 335–349.

Hursán, G., and Zhdanov, M. S., 2002, Contraction integral equation method in three-dimensional electromagnetic modelling: *Radio Science* **37**, 1089–2002. doi: 10.1029/2001RS002513

Kasaya, T., Goto, T., and Takagi, R., 2006, Marine electromagnetic observation technique and its development – for crustal structure survey: *Butsuri-Tansa* **59**, 585–594.

Mittet, R., Maao, F., Aakervik, O. M., and Ellingsrud, S., 2005, A two-step approach to depth migration of low frequency electromagnetic data: 75th Annual International Meeting, SEG, *Expanded Abstracts*, 522–525.

Portniaguine, O., and Zhdanov, M. S., 1999, Focusing geophysical inversion images: *Geophysics* **64**, 874–887. doi: 10.1190/1.1444596

Tada, N., and Seama, K., 2006, Surveys of the oceanic crust resistivity structure using a magnetometric resistivity method: *Butsuri-Tansa* **59**, 171–180.

Tompkins, M. J., 2004, Marine controlled-source electromagnetic imaging for hydrocarbon exploration: interpreting subsurface electrical properties: *First Break* **22**, 27–33.

Ueda, T., and Zhdanov, M. S., 2006, Fast numerical modelling of multitransmitter electromagnetic data using multigrid quasi-linear approximation: *IEEE Transactions on Geoscience and Remote Sensing* **44**, 1428–1434. doi: 10.1109/TGRS.2006.864386

Zhdanov, M. S., 1981, Continuation of nonstationary electromagnetic fields in geoelectrical problems: Izv. Akad. Nauk SSSR: *Fizika Zemly* **12**, 60–69.

Zhdanov, M. S., 1999, Electromagnetic migration: in Deep Electromagnetic Exploration, Springer-Verlag, Narosa Publishing House, 283–298.

Zhdanov, M. S., 2001, Method of broad band electromagnetic holographic imaging: US Patent # 6,253,100 B1.

Zhdanov, M. S., 2002, Geophysical Inverse Theory and Regularization Problems, Elsevier.

Zhdanov, M. S., and Frenkel, M. A., 1983*a*, The solution of the inverse problems on the basis of the analytical continuation of the transient electromagnetic field in reverse time: *Journal of Geomagnetism and Geoelectricity* **35**, 747–765.

Zhdanov, M. S., and Frenkel, M. A., 1983*b*, Electromagnetic migration in Hjelt, S. E., ed., The development of the deep geoelectric model of the baltic shield, Part 2, Univ. of Oulu, Oulu, 37–58.

Zhdanov, M. S., and Fang, S., 1996, Quasi-linear approximation in 3D EM modelling: *Geophysics* **61**, 646–665. doi: 10.1190/1.1443994

Zhdanov, M. S., and Keller, G., 1994, The geoelectrical methods in geophysical exploration: Elsevier.

Zhdanov, M. S., Traynin, P., and Booker, J., 1996, Underground imaging by frequency domain electromagnetic migration: *Geophysics* **61**, 666–682. doi: 10.1190/1.1443995

Zhdanov, M. S., and Traynin, P., 1997, Migration versus inversion in electromagnetic imaging technique: *Journal of Geomagnetism and Geoelectricity* **49**, 1415–1437.

Manuscript received August 10 2007; accepted October 31 2007.

多重格子準線形近似と反復電磁マイグレーションによる海洋人工電流源電磁探査データの高速な数値計算法

上田　匠[1]・M. S. ジュダノフ[2]

要　旨：　海洋人工電流源電磁探査法データの３次元解釈は，複数の送受信機を利用することにより膨大な数値計算量を要求される非常に難しい問題である。この問題に取り組むため，本研究では，海底電磁場受信機と曳航式送信機から構成される一般的な海洋人工電流源電磁探査データ解釈への電磁(EM)マイグレーションの適用を検討した。
また同時に，電磁マイグレーションが複数の送受信配置による海洋人工電流源電磁探査の数値解析への利用に非常に適していることを数値計算により示した。マイグレーション電磁場の導出においては，計算速度向上のため，これまでに著者らが開発した積分方程式法による順解析計算の高速近似型である多重格子準線形(MGQL; multigrid quasi-linear)近似を利用した。本稿で検討した一連のマイグレーション解析法は，一般的な海底石油ガス貯留層探査問題を利用して検証をおこなった。

キーワード：電磁探査，海洋 CSEM，積分方程式，準線形近似，電磁マイグレーション，数値解析，インバージョン

다중격자 준선형 근사 및 반복적 전자탐사 구조보정법에 기초한 해양 인공송신 전자탐사 자료의 빠른 수치해석 기법

Takumi Ueda[1] and Michael S. Zhdanov[2]

요 약: 이 논문에서 우리는 해저용 수신기들과 이동하는 전기적 양극송신기의 한 조로 이루어진 전형적인 해양 인공송신 전자탐사 (MCSEM) 방법에 의해 얻어진 자료 해석에 전자탐사 구조보정법의 적용을 다룬다. 이 연구에서와 같이 다중 송신기와 다중 수신기를 이용해 획득된 자료는 방대한 컴퓨터 계산을 요하기 때문에 MCSEM자료의 3차원적 해석은 매우 도전적인 문제이다. 이와 동시에, 우리는 조밀하게 송신 및 수신기를 위치 시켜야 하는 이 MCSEM시스템은 구조보정법의 적용에 아주 적합하다는 것을 보여줄 것이다. 구조보정장 계산의 속도를 증가시키기 위해 우리는 직접 개발한 다중격자 준선형 (MGQL) 근사법에 기초한 적분방정식 해의 빠른 형태를 적용시켰다. 이 논문에서 공식화된 구조보정 영상 원리는 전형적인 해저 석유 저류층 모델에 적용되어 시험 되었다.

주요어 : 전자탐사, 해양 CSEM, 적분방정식, 준선형 근사, 전자탐사 구조보정, 수치해석법, 역산 문제

１ 産業技術総合研究所 地圏資源環境研究部門
〒305-8567　茨城県つくば市東 1-1-1 中央第 7
２ ユタ大学地質地球物理学科

1 일본 산업기술종합연구소 지구자원환경연구부문

2 미국 유타 대학, 지질 및 지구물리학과